Cawangan Kedah
Kampus Sungai Petani

e-PROCEEDINGS

of The 5th International Conference on Computing, Mathematics and Statistics (iCMS2021)

4-5 August 2021

Driving Research Towards Excellence

e-Proceedings of the 5th International Conference on Computing, Mathematics and Statistics (iCMS 2021)

Driving Research Towards Excellence

Editor-in-Chief: Norin Rahayu Shamsuddin

Editorial team:

Dr. Afida Ahamad
Dr. Norliana Mohd Najib
Dr. Nor Athirah Mohd Zin
Dr. Siti Nur Alwani Salleh
Kartini Kasim
Dr. Ida Normaya Mohd Nasir
Kamarul Ariffin Mansor

e-ISBN: 978-967-2948-12-4
DOI

Library of Congress Control Number:

Publication by
Department of Mathematical Sciences
Faculty of Computer & Mathematical Sciences
UiTM Kedah

TABLE OF CONTENT

PART 1: MATHEMATICS

PART 2: STATISTICS

PART 3: COMPUTER SCIENCE & INFORMATION TECHNOLOGY

PART 4: OTHERS

RADIATION EFFECT ON MHD FERROFLUID FLOW WITH RAMPED WALL TEMPERATURE AND ARBITRARY WALL SHEAR STRESS

Nor Athirah Mohd Zin[1], Aaiza Gul[2], Siti Nur Alwani Salleh[3*], Imran Ullah[4], Sharena Mohamad Isa[5], Lim Yeou Jiann[6] and Sharidan Shafie[7]

[1,3]Faculty Computer and Mathematical Sciences, Universiti Teknologi Mara (UiTM), Cawangan Kedah, Kampus Sungai Petani, 08400, Merbok, Kedah, [2]School of Information, Computer and Communication Technology, Sirindhorn International Institute of Technology, Thammasat University, Rangsit Center, Pathum Thani, Thailand, [4]College of Civil Engineering, National University of Sciences and Technology Islamabad, 44000 Pakistan, [5]Manufacturing Engineering Technology Section, UniKL, Italy Design Institute, Kuala Lumpur, 56100 Malaysia, [6,7]Department of Mathematical Sciences, Faculty of Science, University Teknologi Malaysia, 81310, Skudai Johor.

([1]athirahmz@uitm.edu.my, [2]Aaizagul@gmail.com, [3]sitinuralwanisalleh@uitm.edu.my [4]ullahimran14@gmail.com, [5]sharena@unikl.edu.my, [6]jiann@utm.my and [7]sharidan@utm.my)

This research investigates the effect of thermal radiation on unsteady magnetohydrodynamics free convection flow of ferrofluid over a vertical flat plate with ramped wall temperature and arbitrary wall shear stress. A comparison study between the magnetic nanoparticles iron oxide (Fe_2O_3) and non-magnetic nanoparticles alumina oxide (Al_2O_3) with water-based fluid are constructed. An appropriate dimensionless variables are introduced to the governing equations and solved analytically by using the Laplace transform technique. The variations of the profile for various values of the pertinent parameters are graphically presented and discussed. The results reveal that the velocity and temperature in the ramped wall condition are always lower than in the isothermal situation. Further, the liquid with the non-magnetic nanoparticles has a higher velocity and temperature in either the ramped plate or isothermal plate.

***Keywords*:** Ferrofluid, MHD, Radiation, Ramped Temperature, Exact Solution.

1. Introduction

In 1995, Choi and Eastman experimentally reported in their innovative work that when a small volume of solid nanoparticles was added to a common host fluid, it increased excessively the effective thermal conductivity of the base fluids. The mixtures were called nanofluids. Recent development in nanotechnology shows that it is possible to create new devices and materials with varieties of potential applications, such as biomaterial, Nano-electronics, transportation, and nuclear reactors (Tlili, 2021).

Joseph et al. (2019) investigated the optimisation of thermo-optical properties of nanofluid for direct absorption solar collectors. They considered nanofluid with suspended spherical nanoparticles SiO_2/Ag-CuO in the water-base fluid. Kalantari et al. (2019) and Tahmooressi et al. (2021) acknowledged the enhancement of thermal conductivity of a size-controlled silver nanofluid and simulated the nanoparticles' size/aspect ratio effect on the thermal conductivity of the nanofluids by using the lattice Boltzmann method. Rashid et al. (2021) studied the characteristic of two different types of hybrid nanofluids with different shapes of nanoparticles on the heat transfer and fluid flow toward a stretching/shrinking horizontal cylinder. Nanoparticles of Ag and TiO_2 in the water-based nanofluid were considered in their work at the range of volume fraction $0 \le \varphi \le 0.04$. An interesting investigation was carried out by Anuar et al. (2021) to determine the numerical computation of dusty hybrid nanofluid flow and heat transfer over a deformable sheet with slip effect.

Saqib et al. (2021) deliberated the shape effect on the MHD flow of a time-fractional Ferro-Brinkman type nanofluid under the influence of ramped heating. They have solved the fluid problem analytically via the Laplace transformed method. They considered water as the conventional base fluids which have been suspended by spherical shape magnetic nanoparticles. Another study related hybrid nanofluid, unsteady hybrid nanofluid flow over a radially permeable shrinking/stretching surface was done by Umair et al. (2021). Anwar et al. (2021) applied the Laplace transform technique to solve the fractional $Fe_3O_4 - MoS_2$ -water hybrid nanofluid flow over an inclined surface with the ramped heating and ramped boundary motion.

Of recent, the heat transfer and fluid flow analysis of nanofluid with the interaction of magnetic field have increased enormously. Such kinds of nanofluid have numerous industrial and engineering applications. The slip and radiative effects on the water-based magnetic Fe_3O_4 nanofluid flow over a nonlinearly stretching sheet in a porous media with Soret and Dufour diffusion were numerically examined by Bhatti et al., (2020). Krishna et al. (2021) analyzed the radiation absorption of an MHD convective flow of nanofluids through a vertical movement absorbent plate.

Free convection flows are also of great interest in industrial applications such as granular insulation, fiber, geothermal systems, nuclear reactors, filtration processes, design of spaceship, etc. Soundalgekar (1977) was the first found the exact solution for the free convection flow of a viscous incompressible fluid past an impulsively started infinite vertical plate. Khan and Alzahrani (2021) analyzed the radiation effects on a free convection nanofluid flow (silicon dioxide and molybdenum disulfide) by considering the influence of second-order velocity slip, entropy generation, and Darcy-Forchheimer porous medium. The numerical solution of free convection heat transfer from a concave hemispherical surface was studied by Behera et al. (2021).

The above studies show that no attempt has been made to analyze the radiation effect on the MHD ferrofluid flow with ramped wall temperature and arbitrary wall shear stress. Thus, the present study aims to investigate the behavior of a free convection water-based nanofluid that flows over a vertical plate with ramped wall temperature under the influence of thermal radiation. Besides, the effect of a magnetic field on fluid flow and heat transport is also taken into the consideration. A comparison of non-magnetic nanoparticles with magnetic nanoparticles is conducted. Analytical solutions are obtained through the Laplace transform methods. The interaction of the magnetic field with the magnetite nanoparticles in the free convection nanofluid flow is presented graphically and discussed.

2. Mathematical Formulation

We consider the unsteady MHD free convection flow of an incompressible ferrofluid over an infinite vertical flat plate. The flow being confined to $y > 0$, where y is the coordinate measured in the normal direction to the plate. The fluid is assumed to be electrically conducting with a uniform magnetic field of strength B_0, that is applied in a direction perpendicular to the plate. The magnetic Reynolds number is assumed to be small enough to neglect the effects of the induced magnetic field.

Based on the approximation of Boussinesq and taking into consideration the above assumptions, the governing equations of momentum and energy are obtained as follows:

$$\rho_{nf} \frac{\partial u}{\partial t} = \mu_{nf} \frac{\partial^2 u}{\partial y^2} + g\left(\rho\beta\right)_{nf}\left(T - T_\infty\right) - \sigma_{nf} B_0^2 u, \tag{1}$$

$$\left(\rho c_p\right)_{nf} \frac{\partial T}{\partial t} = k_{nf} \frac{\partial^2 T}{\partial y^2} - \frac{\partial q_r}{\partial y}, \tag{2}$$

subjected to initial and boundary conditions

$$u\left(y,0\right) = 0; \quad T\left(y,0\right) = T_\infty; \quad \forall y \geq 0, \tag{3}$$

$$\frac{\partial u(0,t)}{\partial y} = \frac{f(t)}{\mu_{nf}}; \quad t>0, \quad T(0,t) = \begin{cases} T_\infty + (T_w - T_\infty)\dfrac{t}{t_0}, & 0 < t \le t_0 \\ T_w, & t > t_0 \end{cases}, \tag{4}$$

$$u(\infty,t) = 0; \quad T(\infty,t) = T_\infty; \quad t>0, \tag{5}$$

where $u(y,t)$ is velocity component of the fluid and dust particle phases along the *x*-direction, ρ_{nf} is the density of the nanofluid, μ_{nf} is the coefficient of viscosity of the nanofluid, g is the acceleration due to gravity, $(\rho\beta)_{nf}$ is the thermal expansion coefficient of the nanofluid, σ_{nf} is the electrical conductivity of the nanofluid, $(c_p)_{nf}$ is the specific heat of the nanofluid at constant pressure, T is the temperature of the fluid and k_{nf} is the thermal conductivity of the nanofluid.

By using Rosseland approximation for radiation, the radiation heat flux (Magyari and Pantokratoras, 2011; Muhammad et al., 2020) can be simplified as

$$q_r = -\frac{-4\sigma^*}{3k^*}\frac{\partial T^4}{\partial y}, \tag{6}$$

where σ^* and k^* are Stefan-Boltzman constant and the mean absorption coefficient, respectively. Assuming that the temperature difference within the flow is such that T^4 and may be expanded in Taylor's series. Expanding T^4 about T_∞ and neglecting higher-order, we obtain

$$T^4 \approx 4T_\infty^3 T - 3T_\infty^4. \tag{7}$$

Substituting (6) and (7) into (2), yields

$$(\rho c_p)_{nf}\frac{\partial T}{\partial t} = k_{nf}\frac{\partial^2 T}{\partial y^2} + \frac{16\sigma^* T_\infty^3}{3k^*}\frac{\partial^2 T}{\partial y^2}. \tag{8}$$

The relations of density, dynamic viscosity and thermal conductivity of the nanofluid (Nandkeolyar et al., 2013; Qasim et al., 2014; Devi and Devi, 2016) with the corresponding base fluid are given as

$$\begin{gathered}(\rho c_p)_{nf} = (1-\phi)(\rho c_p)_f + \phi(\rho c_p)_s, \quad \rho_{nf} = (1-\phi)\rho_f + \phi\rho_s; \\ (\rho\beta)_{nf} = (1-\phi)(\rho\beta)_f + \phi(\rho\beta)_s, \quad \mu_{nf} = \frac{\mu_f}{(1-\phi)^{2.5}}, \quad \frac{k_{nf}}{k_f} = \frac{(k_s+2k_f) - 2\phi(k_f-k_s)}{(k_s-2k_f)+\phi(k_f-k_s)},\end{gathered} \tag{9}$$

where ϕ is the volume fraction of the nanoparticles, ρ_f and ρ_s are the densities of the base fluid and solid nanoparticles, $(c_p)_f$ and $(c_p)_s$ are the thermal conductivities of the base fluid and solid nanoparticles, β_f and β_f are the volumetric coefficients of thermal expansions of the base fluid and solid nanoparticles, μ_f is the dynamic viscosity of the base fluid, k_f and k_s are the thermal conductivities of the base fluid and solid nanoparticles.

The thermophysical properties of base fluid and nanoparticles (Loganathan et al., 2013; Qasim et al., 2014; Oztop and Abu-Nada, 2008; Hussanan et al., 2017) are listed in Table 1.

Table 1: Thermophysical properties of base fluid (water) and nanoparticles (iron oxide and alumina oxide)

Model	$c_p\ kg^{-1}K^{-1}$	$\rho\left(kgm^{-3}\right)$	$k\left(Wm^{-1}K^{-1}\right)$	$\beta\times10^{-5}\left(K^{-1}\right)$
H_2O	4179	997.1	0.613	21
Al_2O_3	765	3970	40	0.85
Fe_3O_4	670	5180	9.7	0.5

Now using following dimensionless variables (Khan et al., 2014; Khan et al., 2020; Nandkeolyar et al., 2013)

$$u^*=u\sqrt{\frac{t_0}{\upsilon_f}},\quad y^*=\frac{y}{\sqrt{\upsilon_f t_0}},\quad t^*=\frac{t}{t_0},\quad T^*=\frac{T-T_\infty}{T_w-T_\infty},\quad f^*\left(t^*\right)=\frac{t_0}{\mu_f}f\left(t_0t^*\right),\quad t_0=\frac{\upsilon_f}{U_0^2},\tag{10}$$

so that equations (1) and (8) are reduced to (* notations are dropped for simplicity)

$$\frac{\partial u}{\partial t}=\frac{1}{\phi_1}\frac{\partial^2 u}{\partial y^2}+GrT\phi_3-\frac{M}{\phi_2}u,\tag{11}$$

$$\Pr\frac{\partial T}{\partial t}=\frac{\lambda}{\phi_4}\left[1+\frac{Nr}{\lambda}\right]\frac{\partial^2 T}{\partial y^2}.\tag{12}$$

The corresponding dimensionless initial and boundary conditions are

$$u\left(y,0\right)=0;\quad T\left(y,0\right)=0;\quad \text{for}\quad y\geq 0,\tag{13}$$

$$\frac{\partial u\left(0,t\right)}{\partial y}=\left(1-\phi\right)^{2.5}f\left(t\right);\quad t>0,\quad T\left(0,t\right)=\begin{cases}t & \text{for}\quad 0<t\leq 1\\ 1 & \text{for}\quad t>1\end{cases},\tag{14}$$

$$u\left(\infty,t\right)=0;\quad T\left(\infty,t\right)=0;\quad t>0.\tag{15}$$

Denoting

$$\begin{gathered}\phi_1=\left(1-\phi\right)^{2.5}\left[\left(1-\phi\right)+\phi\frac{\rho_s}{\rho_f}\right],\quad \phi_2=\left(1-\phi\right)+\phi\frac{\rho_s}{\rho_f},\\ \phi_3=\frac{\left(1-\phi\right)\rho_f+\phi\rho_s\left(\frac{\beta_s}{\beta_f}\right)}{\rho_{nf}},\quad \phi_4=\left(1-\phi\right)+\frac{\phi\left(\rho c_p\right)_s}{\left(\rho c_p\right)_f}.\end{gathered}\tag{16}$$

where M is the magnetic parameter, Gr is the Grashof number, $\Pr$ is the Prandtl number and Nr is the radiation parameter which are defined as

$$M=\frac{\sigma_{nf}B_0^2\upsilon_f}{\rho_f U_0^2},\quad Gr=\frac{g\beta_f\upsilon_f\left(T_w-T_\infty\right)}{U_0^3},\quad \Pr=\frac{\upsilon_f\left(\rho c_p\right)_f}{k_f},\quad \lambda=\frac{k_{nf}}{k_f},\quad Nr=\frac{16\sigma^* T_\infty^3}{3k_f k^*}. \tag{17}$$

3. Solution of the Problem

Applying the Laplace transform technique to (11)-(15) and make use of the transformed initial conditions, then we obtained the following differential equations in (*y*,*q*)-plane

$$\frac{1}{\phi_1}\frac{d^2\bar{u}\left(y,q\right)}{dy^2}-\frac{M}{\phi_2}\bar{u}\left(y,q\right)-q\bar{u}\left(y,q\right)+Gr\phi_3\bar{T}\left(y,q\right)=0 \tag{18}$$

$$\frac{\lambda}{\phi_4}\left[1+\frac{Nr}{\lambda}\right]\frac{d^2\bar{T}\left(y,q\right)}{dy^2}-\Pr q\bar{T}\left(y,q\right)=0, \tag{19}$$

with the boundary conditions

$$\frac{d\bar{u}\left(0,q\right)}{dy}=\left(1-\phi\right)^{2.5}F\left(q\right), \tag{20}$$

$$\bar{u}\left(\infty,q\right)=0, \tag{21}$$

$$\bar{T}\left(0,q\right)=\frac{1-e^{-q}}{q^2}, \tag{22}$$

$$\bar{T}\left(\infty,q\right)=0, \tag{23}$$

where $\bar{u}\left(y,q\right)$ and $\bar{T}\left(y,q\right)$ are Laplace transform of $u\left(y,t\right)$ and $T\left(y,t\right)$. Equation (19) subject to the boundary conditions (22) and (23) has the following solution

$$\bar{T}\left(y,q\right)=\left(1-e^{-q}\right)\frac{e^{-y\sqrt{a_0 q}}}{q^2}. \tag{24}$$

Here,

$$a_0=\frac{\Pr\phi_4}{\lambda\left(1+\frac{Nr}{\lambda}\right)}.$$

By taking the inverse Laplace transform of (24) and and using the second shift property, then we obtain

$$T\left(y,t\right)=T_R\left(y,t\right)-T_R\left(y,t-1\right)H\left(t-1\right). \tag{25}$$

Denoting

$$T_R\left(y,t\right)=\left(t+\frac{a_0y^2}{2}\right)\operatorname{erfc}\left(\frac{y}{2}\sqrt{\frac{a_0}{t}}\right)-y\sqrt{\frac{a_0t}{\pi}}e^{-\frac{a_0y^2}{4t}}, \tag{26}$$

where $H\left(t\right)$ is the Heaviside unit step function and $\operatorname{erfc}\left(.\right)$ is the complimentary error function. Then, substituting (24) into (18) and make use of (20) and (21) leads to the following expression

$$
\begin{aligned}
\bar{u}(y,q) &= -\bar{u}_1(q).\bar{u}_4(y,q) - \left(1-e^{-q}\right)\bar{u}_2(q).\bar{u}_4(y,q) + \left(1-e^{-q}\right)\bar{u}_3(q).\bar{u}_5(y,q) \\
&= -\bar{u}_1(q).\bar{u}_4(y,q) + \left(1-e^{-q}\right)\left[-\bar{u}_2(q).\bar{u}_4(y,q) + \bar{u}_3(q).\bar{u}_5(y,q)\right],
\end{aligned} \tag{27}
$$

where

$$
\begin{aligned}
&\bar{u}_1(q) = (1-\phi)^{2.5} F(q), \quad \bar{u}_2(q) = \frac{b_1\sqrt{a_0 q}}{q^2(q-b_2)}, \quad \bar{u}_3(q) = \frac{b_1}{q-b_2}, \\
&\bar{u}_4(y,q) = \frac{e^{-y\sqrt{a_1+\phi_1 q}}}{\sqrt{a_1+\phi_1 q}}, \quad \bar{u}_5(y,q) = \frac{e^{-y\sqrt{a_0 q}}}{q^2},
\end{aligned} \tag{28}
$$

and the arbitrary constants are

$$
a_1 = \frac{M\phi_1}{\phi_2}, \quad b_1 = -\frac{Gr\phi_1\phi_3}{a_0-\phi_1}, \quad b_2 = \frac{a_1}{a_0-\phi_1}.
$$

Then, the inverse Laplace transform of (28) are given by

$$
\begin{aligned}
&u_1(t) = (1-\phi)^{2.5} f(t), \quad u_2(t) = b_1\sqrt{a_0}\left[-\frac{2}{b_2}\sqrt{\frac{t}{\pi}} + \frac{e^{b_2 t}\operatorname{erf}\left(\sqrt{b_2 t}\right)}{b_2^{\frac{3}{2}}}\right], \\
&u_3(t) = b_1 e^{b_2 t}, \quad u_4(y,t) = \frac{e^{-\left(m_1 t + \frac{y^2\phi_1}{4t}\right)}}{\sqrt{\phi_1 \pi t}}, \quad u_5(y,t) = \left(\frac{a_0 y^2}{2} + t\right)\operatorname{erfc}\left(\frac{y}{2}\sqrt{\frac{a_0}{t}}\right) - y\sqrt{\frac{a_0 t}{\pi}}e^{-\frac{y^2 a_0}{4t}}.
\end{aligned} \tag{29}
$$

Here, $\operatorname{erf}(.)$ is the error function and

$$
m_1 = \frac{a_1}{\phi_1}.
$$

Finally, by using the second shift property in (27), the velocity distribution $u(y,t)$ can be written as

$$
u(y,t) = u_a(y,t) + u_R(y,t) - u_R(y,t)H(t-1). \tag{30}
$$

In which $u_a(y,t)$ and $u_R(y,t)$ can be found by using the convolution theorem

$$
\begin{aligned}
u_a(y,t) &= -(u_1 \otimes u_4)(t) \\
&= -\int_0^t u_1(t-s)u_4(y,s)\,ds \\
&= -\frac{(1-\phi)^{2.5}}{\sqrt{\phi_1\pi}}\int_0^t \frac{f(t-s)}{\sqrt{s}} e^{-\left(m_1 s + \frac{y^2\phi_1}{4s}\right)} ds,
\end{aligned} \tag{31}
$$

$$
\begin{aligned}
u_R(y,t) &= -(u_2 \otimes u_4)(t) + (u_3 \otimes u_5)(t) \\
&= -\int_0^t u_2(t-s)u_4(y,s)\,ds + \int_0^t u_3(t-s)u_5(y,s)\,ds \\
&= -b_1\sqrt{\frac{a_0}{\pi\phi_1}}\int_0^t \frac{1}{\sqrt{s}} e^{-\left(m_1 s+\frac{y^2\phi_1}{4s}\right)}\left[-\frac{2}{b_2}\sqrt{\frac{t-s}{\pi}}+\frac{e^{b_2(t-s)}\operatorname{erf}\left(\sqrt{b_2(t-s)}\right)}{b_2^{\frac{3}{2}}}\right]ds \\
&\quad +\int_0^t b_1 e^{b_2(t-s)}\left[\left(\frac{y^2 a_0}{2}+s\right)\operatorname{erfc}\left(\frac{y}{2}\sqrt{\frac{a_0}{s}}\right)-y\sqrt{\frac{a_0 s}{\pi}}e^{-\frac{y^2 a_0}{4s}}\right]ds.
\end{aligned} \tag{32}
$$

3.1 Solution for an Isothermal Plate

It is worth that to compare the obtained results in (25) and (30) with an isothermal case or constant wall temperature. Therefore, the solution of velocity and temperature distributions for an isothermal plate are

$$
\begin{aligned}
u(y,t) = &-\frac{(1-\phi)^{2.5}}{\sqrt{\phi_1\pi}}\int_0^t \frac{f(t-s)}{\sqrt{s}} e^{-\left(m_1 s+\frac{y^2\phi_1}{4s}\right)}ds \\
&-b_1\sqrt{\frac{a_0}{b_2\phi_1\pi}}\int_0^t \frac{1}{\sqrt{s}} e^{b_2(t-s)-\left(m_1 s+\frac{y^2\phi_1}{4s}\right)}\operatorname{erf}\left(\sqrt{b_2(t-s)}\right)ds \\
&+b_1\int_0^t e^{b_2(t-s)}\operatorname{erfc}\left(\frac{y}{s}\sqrt{\frac{a_0}{s}}\right)ds,
\end{aligned} \tag{27}
$$

$$
T(y,t) = \operatorname{erfc}\left(\frac{y}{2}\sqrt{\frac{a_0}{t}}\right). \tag{28}
$$

4. Result and Discussion

The combined effects of radiation and magnetic field on Ferrofluid flow through a vertical plate with ramped wall temperature have been studied. The governing partial differential equations are solved analytically by the Laplace transform technique. The effects of the involved parameters on the fluid field and heat transfer are analyzed graphically and presented in Figures 1-6.

Figure 1 illustrates the influence of nanoparticle volume fraction ϕ on the velocity profile of the Fe_3O_4-water nanofluid. It is found that the velocity of the nanofluid decreases with the increment of the volume fraction. This is because the increase of volume fraction leads to a larger viscosity of the nanofluid result in more resistance to the fluid flow. This nature is observed either in the situation of the ramped wall or isothermal plate. Furthermore, the ramped wall velocity is smaller as compared to the isothermal case.

Figure 2 shows the effect of magnetite and non-magnetite nanoparticles on the velocity of the ferrofluid. It is observed that the velocity of Al_2O_3-water-based nanofluid is greater than the Fe_3O_4-water-based nanofluid. This implies that the Fe_3O_4-water-based nanofluid is more viscous than the Al_2O_3-water-based nanofluid. It is also noticed that the thermal conductivity of the Fe_3O_4-water-based nanofluid is greater than Al_2O_3-water-based nanofluid. Besides, the isothermal case is also compared with the ramped wall case and a greater velocity is detected in the condition of ramped wall either for Al_2O_3 or Fe_3O_4 water-based nanofluid.

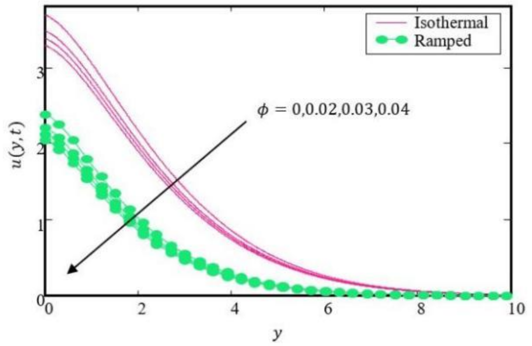

Figure 1: Velocity profile for ϕ when $\mathrm{Pr} = 0.71$, $Gr = 10$, $M = 2$, $Nr = 4$, $f = -0.25$ and $t = 1$.

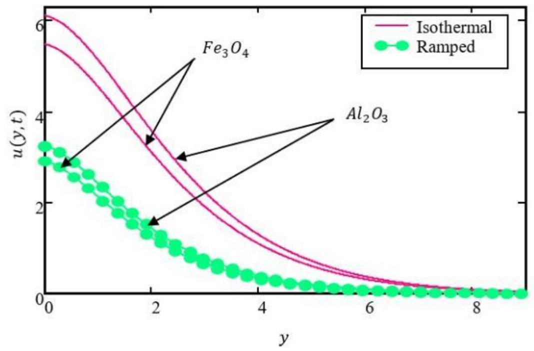

Figure 2: Comparison between magnetic (Fe_3O_4) and non-magnetic (Al_2O_3) nanoparticles when $\phi = 0.04$, $\mathrm{Pr} = 0.71$, $Gr = 10$, $M = 2$, $Nr = 4$, $f = -0.25$ and $t = 1$.

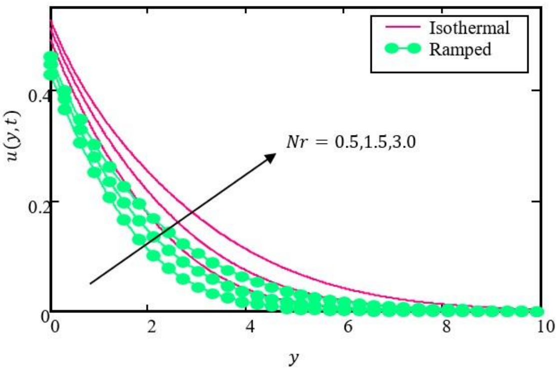

Figure 3: Velocity profile for Nr when $\mathrm{Pr} = 0.71$, $Gr = 1$, $f = -0.25$, $M = 2$, $\phi = 0.04$ and $t = 1.5$.

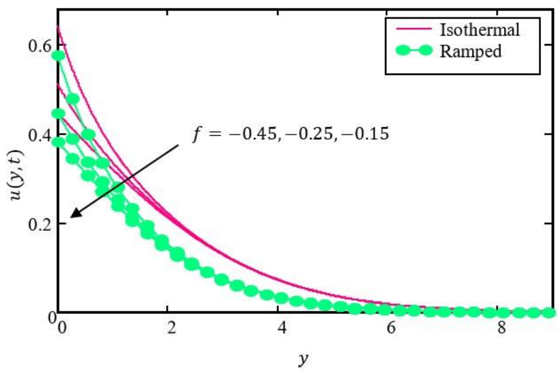

Figure 4: Velocity profile for f when $\mathrm{Pr} = 0.71$, $Gr = 1$, $Nr = 1.5$, $M = 2$, $\phi = 0.04$ and $t = 1.5$.

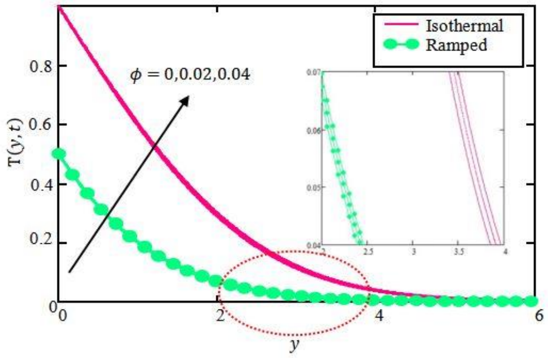

Figure 5: Temperature profile for ϕ when $\mathrm{Pr} = 0.71$, $Nr = 1.5$ and $t = 1.5$.

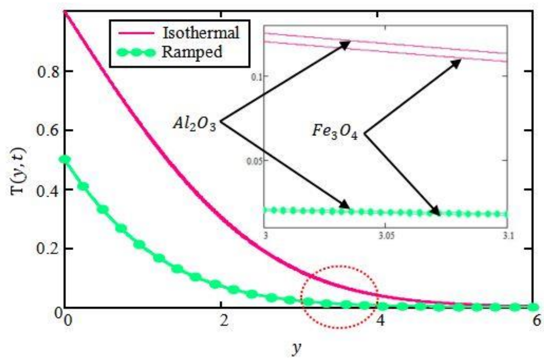

Figure 6: Comparison between magnetic (Fe_3O_4) and non-magnetic (Al_2O_3) nanoparticles when $\phi = 0.04$, $\mathrm{Pr} = 0.71$, $Nr = 1.5$ and $t = 0.5$.

Figure 3 is plotted to show the effect of radiation parameter Nr on the velocity of magnetite nanofluid. It is noticed that the velocity of the Ferrofluid is enhanced with the increase of Nr. This is because increasing the value of radiation parameter will increase the heat conduction which in turn increases the rate of energy transport in the fluids. Thus, decreases the viscosity and thermal conductivity of the Ferrofluid. This will make the fluid move faster and increase the velocity of the Ferrofluid. Meanwhile, Figure 4 depicts the effect of wall shear stress parameter f on the velocity of the Ferrofluid. The figure displays that the velocity decline when the number of f is increased for both isothermal and ramped situations.

Figure 5 demonstrates the temperature distribution for different values of the volume fractions ϕ for isothermal and ramped conditions. The temperature has shown a positive effect on the volume fraction. Physically, the increment of the volume fraction tends to increase the thermal conductivity. Thus, the enhancement of the thermal conductivity has increased the rate of heat transfer and then increase the distribution of the temperature in the fluid. The influence of the volume fraction on the temperature profile either in the isothermal or ramped wall is the same but the temperature is larger in the isothermal situation as compared with the ramped temperature.

Lastly, the graphical results of the temperature profiles for the magnetite and non-magnetite nanoparticles are presented in Figure 6, for both isothermal and ramped plate conditions. The variation of the magnetite and non-magnetite nanoparticles with isothermal and ramped temperatures is very small, almost negligible in ramp temperature. The temperature of non-magnetite nanoparticles is greater than the magnetite nanoparticles. The thermal conductivity and viscosity of the Ferrofluid are temperature dependent. The thermal conductivity increases with the temperature whereas viscosity decreases with the temperature. Therefore, the magnetite nanofluid is more viscous and has a lower temperature as compared to the non-magnetite nanofluid.

5. Conclusion

The present study discusses the combined effects of radiation and magnetic field on the boundary layer flow of a Ferrofluid over a ramped wall temperature vertical plate. Magnetite nanoparticles $\mathrm{Fe_3O_4}$ are suspended inside the conventional water-based fluid. Non-magnetite, $\mathrm{Al_2O_3}$ nanoparticles are chosen for comparison with the magnetite nanoparticles, $\mathrm{Fe_3O_4}$. Moreover, spherical-shaped nanoparticles are considered in this study. It is found that an increase in the volume fraction ϕ of the nanoparticle has increased the viscosity of the nanofluid, which leads to a decrease in the velocity of the magnetite nanofluid. An opposite tendency is observed for the temperature profile with the volume fraction ϕ of the nanoparticle. The fluids with the magnetite nanoparticles are more viscous as compared to the non-magnetite nanofluid due to the greater velocity and temperature that have been detected in the fluid containing $\left(\mathrm{Al_2O_3}\right)$. Lastly, it is noticed that the radiation parameter, Nr is an increasing function of the velocity. The influence of this parameter is found similar in the case of temperature. Furthermore, it is recommended that to consider mass transfer with other relevant effects such as porous medium, inclined magnetic field or Newtonian heating in order to expand the possibilities of this study.

Acknowledgment

We would like to thank the anonymous reviewers for suggestions and helpful comments to improve the manuscript.

References

Anwar, T., Kumam, P., and Thounthong, P. (2021). Fractional modeling and exact solutions to analyze thermal performance of Fe_3O_4-MoS_2- Water hybrid nanofluid flow over an inclined surface with ramped heating and ramped boundary motion. *IEEE Access*, 9:12389-12404.

Anuar, N. S., Bachok, N., and Pop, I. (2021). Numerical computation of dusty hybrid nanofluid flow and heat transfer over a deformable sheet with slip effect. *Mathematics*, 9(643): 1-18.

Behera, B. R., Chandrakar, V. and Senapati, J. R. (2021). Free convection in heat transfer from a concave hemispherical surface: A numerical exercise. *International communications in heat and mass transfer*,125.

Bhatti, M. M., Khalique, C. M., Bég, T. A., Bég, O. A., and Kadir, A. (2020). Numerical study of slip and radiative effects on magnetic Fe_3O_4 -water-based nanofluid flow from a nonlinear stretching sheet in porous media with Soret and Dufour diffusion. *Modern Physics Letters B*, 34(02): 2050026.

Choi, S. U. S. and Eastman, J. A. (1995). Enhancing thermal conductivity fluids with nanoparticles, 66:99-105. IMECE 2016.

Devi, S. S. U. and Devi, S. P. A. (2016). Numerical investigation of three-dimensional hybrid Cu-Al_2O_3/water nanofluid flow over a stretching sheet with effecting Lorentz force subject to newtonian heating. *Canadian Journal of Physics*, 94(5): 490-496.

Hussanan, A., Salleh, M. Z., Khan, I. and Shafie, S. (2017). Convection heat transfer in micropolar nanofluids with oxide nanoparticles in water, kerosene and engine oil. *Journal of Molecular Liquids*. 229: 482-488.

Joseph, A., Sreekumar, S., Kumar, C. S., and Thomas, S. (2019). Optimisation of thermo-optical properties of SiO2/Ag–CuO nanofluid for direct absorption solar collectors. *Journal of Molecular Liquids*, 296: 111986.

Krishna, M. V., Ahamad, N. A., and Chamkha, A. J. (2021). Radiation absorption on MHD convective flow of nanofluids through vertically travelling absorbent plate. *Ain Shams Engineering Journal*.

Kalantari, A., Abbasi, M., and Hashim, A. M. (2019). Enhancement of thermal conductivity of size controlled silver nanofluid. *Materials Today: Proceedings*, 7:612-618.

Khan, M. I., and Alzahrani, F. (2021). Free convection and radiation effects in nanofluid (silicon dioxide and molybdenum disulfide) with second order velocity slip, entropy generation, Darcy-Forchheimer porous medium. *International Journal of Hydrogen Energy*, 46(1):1362-1369.

Khan, A., Khan, I. and Khan, D. (2020). MHD rotating fluid flow past a vertical plate that applies arbitrary shear stress with ramped wall temperature. *International Journal of Computational Analysis*, 3(2):1-15.

Khan, A., Khan, I., Ali, F., Ulhaq, S. and Shafie, S. (2014). Effects of wall shear stress on unsteady MHD conjugate flow in a porous medium with ramped wall temperature. *PLoS ONE*. 9(3):1-12.

Loganathan, P., Nirmal Chand, P. and Ganesan, P. (2013). Radiation effects on an unsteady natural convective flow of a nanofluid past an infinite vertical plate. *Nano: Brief Reports and Reviews*, 8(1):1-10.

Magyari, E. and Pantokratoras, A. (2011). Note on the effect of thermal radiation in the linearized Rosseland approximation the heat transfer characteristics of various boundary layer flows. *International Communications in Heat and Mass Transfer*, 38: 554-556.

Muhammad, T., Waqas, H., Khan, S. A., Ellahi, R. and Sait, S. M. (2020). Significance of nonlinear thermal radiation in 3D Eyring-Powell nanofluid flow with Arrhenius activation energy. *Journal of Thermal Analysis and Calorimetry*.

Nandkeolyar, R., Das, M. and Pattnayak, H. (2013). Unsteady hydromagnetic radiative flow of a nanofluid past a flat plate with ramped temperature. *Journal of the Orissa Mathematical Society*, 32(1): 15-30.

Oztop, H. F. and Abu-Nada, E. (2008). Numerical study of natural convection in partially heated rectangular enclosures filled with nanofluids. *International Journal of Heat and Fluid Flow*, 29 (5): 1326-1336.

Qasim, M., Khan, Z. H., Khan, W. A. and Ali Syah, I. (2014). MHD boundary layer slip flow and heat transfer of Ferrofluid along a stretching cylinder with prescribed heat flux. *PLoS ONE*, 9(1): 1-6.

Rashid, U., Liang, H., Ahmad, H., Abbas, M., Iqbal, A., and Hamed, Y. S. (2021). Study of (Ag and TiO2)/water nanoparticles shape effect on heat transfer and hybrid nanofluid flow toward stretching shrinking horizontal cylinder. *Results in Physics*, 21:103812.

Saqib, M., Khan, I., Shafie, S., and Mohamad, A. Q. (2021). Shape effect on MHD flow of time fractional Ferro-Brinkman type nanofluid with ramped heating. *Scientific reports*, 11(1):1-22.

Soundalgekar, V. M. (1977). Free convection effects on the flow past an infinite vertical oscillating plate. *Astrophysics and space science*, 64(1):65-171.

Tahmooressi H., Kasaeian, A., Yavarinasab, A., Tarokh, A., Ghazi, M. and Hoorfar, M. (2021). Numerical simulation of nanoparticles size/aspect ratio effect on thermal conductivity of nanofluids using lattice Boltzmann method. *International Communications in Heat and Mass Transfer*, 120.

Tlili, I. (2021). Impact of thermal conductivity on the thermophysical properties and rheological behavior of nanofluid and hybrid nanofluid. *Mathematical Sciences*, 1-9.

Umair, I., Waini, I., Ishak, A. and Pop, I. (2021). Unsteady hybrid nanofluid flow over a radially permeable shrinking/stretching surface. *Journal of Molecular Liquids*, 331.

2021 ICMS

INTERNATIONAL CONFERENCE ON COMPUTING, MATHEMATICS AND STATISTICS

e ISBN 978-967-2948-12-4

9 7 8 9 6 7 2 9 4 8 1 2 4